

Reactive Power and Voltage Control in Distribution Systems with Limited Switching Operations

M. B. Liu, Claudio A. Cañizares, *Fellow, IEEE*, and W. Huang

Abstract—An algorithm based on a nonlinear interior-point method and discretization penalties is proposed in this paper for the solution of the mixed integer nonlinear programming (MINLP) problem associated with reactive power and voltage control in distribution systems to minimize daily energy losses, with time-related constraints being considered. Some of these constraints represent limits on the number of switching operations of transformer load tap changers (LTCs) and capacitors, which are modeled as discrete control variables. The discrete variables are treated here as continuous variables during the solution process, thus transforming the MINLP problem into an NLP problem that can be more efficiently solved exploiting its highly sparse matrix structure; a strategy is developed to round these variables off to their nearest discrete values, so that daily switching operation limits are properly met. The proposed method is compared with respect to other well-known MINLP solution methods, namely, a genetic algorithm and the popular GAMS MINLP solvers BARON and DICOPT. The effectiveness of the proposed method is demonstrated in the well-known PG&E 69-bus distribution network and a real distribution system in the city of Guangzhou, China, where the proposed technique has been in operation since 2003.

Index Terms—Distribution systems, reactive power control, voltage control, optimal switching operations, mixed integer nonlinear programming, nonlinear programming, interior point methods, genetic algorithms, optimization solvers.

I. INTRODUCTION

Reactive power and voltage control in distribution systems is typically associated with the optimal hourly adjustment of transformer taps and capacitor banks, so that daily energy losses are minimized, while satisfying operating constraints based on the load forecasted a day ahead. Due to transformer load tap changers (LTCs) and circuit breaker manufacturer restrictions, and to increase their life expectancy, frequent switching operations of LTCs and capacitor banks should be prevented. Thus, optimal reactive power and voltage control in distribution systems requires the solution of an optimization problem for the 24 hours of the day before the dispatch day to minimize the daily system losses, while limiting the number of LTC and capacitor bank hourly switching operations [1, 2].

Various algorithms have been proposed to solve the aforementioned reactive power and voltage control

optimization problem, which is basically a non-convex, mixed-integer nonlinear programming (MINLP) problem, due to the discrete nature of the LTC and capacitor bank switching, as well as the nonlinear power flow constraints. In [1]-[4], a dynamic programming approach combined with fuzzy sets or artificial neural networks is applied to the determination of optimal switching schedules in a 24h period for capacitors along feeders and transformers and capacitors in a distribution substation. However, in these articles, in order to obtain a reasonable solution in a given time window, the solution space is simplified using some heuristics. In [5], the distribution network is divided into two parts, namely, feeders and substation; the switching sequence of capacitors in each feeder is first determined using a dynamic programming approach, and then the dispatch schedules of capacitors and transformers in a substation are obtained using a dynamic programming approach as well. In [6], the problem is decomposed into the same two sub-problems as in [5], i.e. the dispatch schedule of transformers and capacitors in a substation and the schedule of the feeder capacitors; these sub-problems are solved using a simplified dynamic programming approach and a fuzzy control algorithm, respectively, and then a coordination strategy between these two is proposed. Since the solution space increases rapidly with system size, dynamic programming approaches are not really suitable for large-scale distribution networks.

Other techniques have also been proposed in the literature, considering a maximum allowable daily switching operation number (MADSON) of the control devices. For example, the authors in [7] divide the load curve into several segments according to the distribution of losses at each hour, and then convert this into an equivalent staircase curve based on an equal-area criterion, in which the numbers of steps satisfy a given MADSON constraint. By means of this mechanism, the multi-period optimization model is transformed into several single-period models; however, an extra limitation is imposed in the number of simultaneous operations of control devices, with all having to operate or stop synchronously in a given time interval. In [8], an integrated reactive power optimization model is proposed, with the switching sequence of transformers and capacitors being determined first based on heuristic rules, and then transforming the multi-period optimization model into several single-period models that can be readily solved via “conventional” optimization algorithms. The authors in [9] propose a time-interval based control strategy, decomposing the daily load curve into several sequential load levels, with the number of levels being equal to the capacitors’ MADSON; a genetic algorithm is used to determine both the load level partition and the dispatch schedule. In [10], a fuzzy-based reactive power optimization model is proposed and tested in a real distribution network; the model considers constraints in the number of switching

This work was supported in part by the National Science Foundation of China under Grant No. 50777021.

M. B. Liu is with Electric Power College, South China University of Technology, Guangzhou, Guangdong, China (e-mail: epmbliu@scut.edu.cn).

Claudio A. Cañizares is with Department of Electrical and Computer Engineering, University of Waterloo, Ontario, Canada (e-mail: ccanizar@uwaterloo.ca).

W. Huang is with the Foshan Power Supply Bureau of Guangdong Power Grid Inc., Foshan, Guangdong Province, China (e-mail: norchy@163.com).

operation of control devices, and a simulated annealing search technique is used to solve the problem.

In this paper, a novel approach for the solution of the optimal reactive power and voltage control problem in distribution networks with MADSON constraints is proposed and discussed. The proposed technique tries to address some of the shortcomings of the previously described methodologies, in particular the issue of efficiently obtaining reasonable solutions for realistic distribution networks, while avoiding simplifying assumptions/approximations in the treatment of the discrete control devices. The method proposed in [11] for handling discrete variables in a classical loss-minimization optimal power flow or OPF problem, where the discrete variables are transformed into continuous variables by mean of a round-off algorithm, is applied here to efficiently obtain solutions for a complex and large multi-period optimization problem encountered in practice in distribution systems. The sparse-matrix structure of the resulting optimization problem is fully exploited to enhance the solution efficiency and allow its practical application. The effectiveness of the proposed methodology is demonstrated through the results obtained from applying it to a widely studied distribution system and a real distribution network in China, where the method has been implemented and is in operation since 2003, comparing it with three other known techniques for the solution of MINLP problems of the kind discussed here, namely, a genetic algorithm [12, 13], and the GAMS solvers BARON 7.2.5 and DICOPT++ [14].

The rest of paper is structured as follows: Section II describes the MINLP model used for reactive power and voltage control, and the proposed solution technique is presented and discussed in Section III. Section IV briefly describes the genetic algorithm and the GAMS' BARON and DICOPT solvers used here for comparison, and Section V discusses and compares the results obtained for the well-known PG&E 69-bus distribution network and a real distribution system in Guangzhou, China, where the MADSON for LTCs and capacitor banks is an issue. Finally, a summary and the main contributions of the paper are presented in Section VI.

II. PROBLEM FORMULATION

The reactive power and voltage control problem in a distribution system can be cast, for a 24 h period, as the following optimization problem, considering that active and reactive power load levels are available from a load forecast process:

$$\min \quad E = \sum_{t=0}^{23} f(x_{1(t)}, x_{2(t)}, x_{3(t)}) \quad (1)$$

$$\text{s.t.} \quad g(x_{1(t)}, x_{2(t)}, x_{3(t)}) = 0 \quad \forall t \quad (2)$$

$$x_{1(t)\min} \leq x_{1(t)} \leq x_{1(t)\max} \quad \forall t \quad (3)$$

$$x_{2(t)\min} \leq x_{2(t)} \leq x_{2(t)\max} \quad \forall t \quad (4)$$

$$h(x_{1(0)}, x_{1(1)}, \dots, x_{1(23)}) = \sum_{t=0}^{23} |x_{1(t+1)} - x_{1(t)}| \leq S_{x_1} C_{x_1} \quad (5)$$

where:

E daily energy loss;

$x_{1(t)}$ discrete control variables, i.e. capacitor bank and transformer tap settings at hour t , $x_{1(t)} \in \mathbb{R}^p$, and $p = r + u$;

$x_{2(t)}$ injected reactive powers at the slack bus and bus voltage magnitudes at hour t , $x_{2(t)} \in \mathbb{R}^q$, and $q = n + 1$;

$x_{3(t)}$ injected active powers at the slack bus and bus voltage angles except for the slack bus at hour t , $x_{3(t)} \in \mathbb{R}^n$;

C_{x_1} vector of MADSON of capacitor banks and transformer LTCs, $C_{x_1} \in \mathbb{R}^p$;

S_{x_1} diagonal matrix formed by the step sizes of capacitor bank and transformer tap settings, $S_{x_1} \in \mathbb{R}^{p \times p}$;

n number of buses;

u number of LTC transformers;

r number of capacitor banks.

The objective function f in (1) represents the active-power loss at hour t , and (2) stands for the nonlinear power-flow equations for all 24 hours ($t = 0, 1, 2, \dots, 23$). Inequality constraints (3) and (4) define the feasibility region of the problem variables, while inequality constraints (5) correspond to daily limits on the number of switching operations of capacitor banks and transformer LTCs. In (5), the number of switching operations for each device in an hour t is defined as the number of steps a capacitor bank switches on or off, or the number of tap positions an LTC moves; hence, the number of switching operations of a capacitor bank or LTC in an hour can be expressed using the modulus of the total change on capacitance or tap setting divided by the corresponding step size, which is assumed uniform here, without loss of generality.

III. SOLUTION ALGORITHM

Following standard solution optimization approaches, slack variables are introduced to transform the inequality constraints (3)-(5) into the following equality constraints:

$$x_{1(t)} + s_{u1(t)} = x_{1(t)\max} \quad (6)$$

$$x_{1(t)} - s_{l1(t)} = x_{1(t)\min} \quad (7)$$

$$x_{2(t)} + s_{u2(t)} = x_{2(t)\max} \quad (8)$$

$$x_{2(t)} - s_{l2(t)} = x_{2(t)\min} \quad (9)$$

$$h(x_{1(0)}, x_{1(1)}, \dots, x_{1(23)}) + s_n = S_{x_1} C_{x_1} \quad (10)$$

$$s_{u1(t)}, s_{l1(t)}, s_{u2(t)}, s_{l2(t)}, s_n \geq 0 \quad (11)$$

Where $s_{u1(t)}$, $s_{l1(t)}$, $s_{u2(t)}$, $s_{l2(t)}$, and s_n are slack variables; $s_{u1(t)}$, $s_{l1(t)}$, $s_n \in \mathbb{R}^p$, and $s_{u2(t)}, s_{l2(t)} \in \mathbb{R}^q$. Thus, the original model (1)-(5) is transformed into an equivalent model consisting of (1), (2) and (6)-(11).

The capacitor bank and transformer tap settings are defined by discrete variables. The value of a discrete variable x_b is determined by its step size; for example, if the full capacity of a given capacitor bank is 1200 kvar, and there are 4 sets of equal capacity, each step size is hence 300 kvar. In this paper, these discrete variables are handled by means of penalty

functions, similarly to what was proposed in [11] for handling discrete variables for a different optimization problem. Therefore, based on an interior point method (IPM) approach [15], it is assumed here that each discrete variable has its own uniform step size. Thus, a neighborhood $R(x_{b1})$ of a discrete value x_{b1} can then be defined as:

$$R(x_{b1}) = \left\{ x_b \mid x_b - \frac{1}{2}d \leq x_b \leq x_{b1} + \frac{1}{2}d \right\} \quad (12)$$

where d is the step size of the discrete variable x_b , and x_{b1} is its neighborhood centre. During the IPM iterations, x_b is driven towards its neighborhood centre using the following quadratic penalty function:

$$\varphi(x_b) = \frac{1}{2} \nu_b (x_b - x_{b1})^2 \quad (13)$$

where ν_b is the penalty factor. It should be noted that the neighborhood centre of x_b , which may change dynamically between iterations, is determined by rounding off the value of x_b to its nearest discrete value.

Applying an IPM, a Lagrangian function associated with equality constraints (2) and (6)-(10), using logarithmic barrier functions to eliminate the non-negativity constraints of slack variables in (11), and quadratic penalty functions (13) to handle all discrete variables, can be defined as follows:

$$L = \sum_{t=0}^{23} \left\{ L_t + \frac{1}{2} \sum_{j=1}^p \nu_{j(t)} (x_{1(t)j} - x_{1(t)jb})^2 \right\} - y_n^T [h(x_{1(0)}, x_{1(1)}, \dots, x_{1(23)}) + s_n - S_{x_i} C_{x_i}] - \mu \sum_{j=1}^p \ln s_{nj} \quad (14)$$

where

$$L_t = f(x_{1(t)}, x_{2(t)}, x_{3(t)}) - y_{(t)}^T g(x_{1(t)}, x_{2(t)}, x_{3(t)}) - y_{u1(t)}^T (x_{1(t)} + s_{u1(t)} - x_{1(t)\max}) - y_{l1(t)}^T (x_{1(t)} - s_{l1(t)} - x_{1(t)\min}) - y_{u2(t)}^T (x_{2(t)} + s_{u2(t)} - x_{2(t)\max}) - y_{l2(t)}^T (x_{2(t)} - s_{l2(t)} - x_{2(t)\min}) - \mu \sum_{j=1}^p (\ln s_{u1(t)j} + \ln s_{l1(t)j}) - \mu \sum_{j=1}^q (\ln s_{u2(t)j} + \ln s_{l2(t)j}) \quad (15)$$

the y 's are the corresponding Lagrangian multipliers for the equality constraints (2) and (6)-(10); $\nu_{j(t)}$ is the discretization penalty factor for discrete variables $x_{1(t)j}$, and $x_{1(t)jb}$ is the corresponding neighborhood center; and $\mu \geq 0$ is the barrier function penalty parameter.

The standard IPM solution approach is based on the Karush-Kuhn-Tucker (KKT) conditions for (14), which in turn require the derivatives of $h(x_{1(0)}, x_{1(1)}, \dots, x_{1(23)})$ with respect to $x_{1(t)} \forall t$. Hence, from (5), one has that:

$$\frac{\partial h_i}{\partial x_{1j(t)}} = \begin{cases} 0 & \text{for } i \neq j \\ \frac{\partial (|x_{1i(t)} - x_{1i(t-1)}| + |x_{1i(t+1)} - x_{1i(t)})}{\partial x_{1i(t)}} & \text{for } i = j \end{cases} \quad (16)$$

Thus:

$$\frac{\partial h_i}{\partial x_{1i(t)}} = \begin{cases} 2 & \text{if } x_{1i(t)} > x_{1i(t-1)} \text{ and } x_{1i(t)} > x_{1i(t+1)} \\ -2 & \text{if } x_{1i(t)} < x_{1i(t-1)} \text{ and } x_{1i(t)} < x_{1i(t+1)} \\ 0 & \text{otherwise} \end{cases} \quad (17)$$

Therefore, one can define the diagonal matrix $M_t \in \mathbb{R}^{p \times p}$,

with its diagonal elements being $\partial h / \partial x_{1(t)}$, which have values $-2, 0$, or 2 during the iterative solution process.

Applying a Newton-Raphson method to solve the KKT conditions, as shown in detail in the Appendix, the following matrix equation needs to be solved at each iteration:

$$\begin{bmatrix} A_{(0,0)} & 0 & \dots & 0 & A_{(0,n)} \\ 0 & A_{(1,1)} & \dots & 0 & A_{(1,n)} \\ \dots & \dots & \dots & \dots & \dots \\ 0 & 0 & \dots & A_{(23,23)} & A_{(23,n)} \\ A_{(n,0)} & A_{(n,1)} & \dots & A_{(n,23)} & A_{(n,n)} \end{bmatrix} \begin{bmatrix} \Delta z_{(0)} \\ \Delta z_{(1)} \\ \dots \\ \Delta z_{(23)} \\ \Delta y_n \end{bmatrix} = \begin{bmatrix} b_{(0)} \\ b_{(1)} \\ \dots \\ b_{(23)} \\ b_n \end{bmatrix} \quad (18)$$

where $A_{(t,t)} \in \mathbb{R}^{(p+q+3n) \times (p+q+3n)} \forall t$ are symmetric matrices,

$b_{(t)} \in \mathbb{R}^{p+q+3n}$, and $\Delta z_{(t)} = [\Delta x_{1(t)} \quad \Delta x_{2(t)} \quad \Delta x_{3(t)} \quad \Delta y_{(t)}]^T$.

The matrices $A_{(t,t)}$, $A_{(n,t)}$, $A_{(t,n)}$ and $A_{(n,n)}$, and the vectors $b_{(t)}$ and b_n are defined in the Appendix, where it is shown that the elements of $A_{(t,t)} \forall t$ are zero, except for the elements in the diagonal and in the last row and column, i.e. the matrix has similar topology as (18). Therefore, even though the dimension of the A matrices increase substantially with system size, this particular sparse matrix structure can be readily exploited to efficiently solve (18) [16].

The proposed IPM solution algorithm can be summarized as follows:

1. Initialize all variables and set the iteration counter $k = 0$, defining the tolerances ε_1 and ε_2 for the IPM complementary gap G_{gap} and the maximum mismatch M_{max} of the power-flow equations (2), respectively (from a variety of tests, $\varepsilon_1 = 10^{-6}$ and $\varepsilon_2 = 10^{-4}$ worked well). For simplicity and without loss of generality, the MADSON for both capacitors and transformers are assumed here to be the same. The discretization penalty factors ν_b are also defined at this stage, considering that, as discussed in [11]:
 - The best values mainly depend on the step sizes of capacitors and transformers, and are independent of the system characteristics; hence, if the step sizes are uniform, as assumed here, these remain constant during the iterative process.
 - The values should not be too large as to affect the progressive improvement of the objective function.
 - Since transformers have smaller step sizes, the values of their penalty factors ν_T should be larger than the penalty factors ν_C for the capacitors, so that the sensitivity of the discretization penalty function (13) is similar for both discrete devices. Multiple tests have shown that the values $\nu_T = 500$ and $\nu_C = 100$ are suitable in most cases.
2. Compute G_{gap} and M_{max} , and if $G_{\text{gap}} < \varepsilon_1$ and $M_{\text{max}} < \varepsilon_2$, then stop the iteration process.
3. Compute the barrier function penalty parameter μ .
4. Determine if the discrete variables violate their limits. If they do, then set the corresponding discretization penalty function factors to zero, and set the corresponding discrete variable values at their limits.
5. If $G_{\text{gap}} < 0.01$, and changes of discrete variables in two consecutive iterations is less than the 1/8 of their corresponding step sizes (these particular values have been chosen based on multiple tests), then determine the

corresponding neighborhood centers. If they do not satisfy these criteria, then set their penalty factors to zero.

6. Solve equations (18) to obtain the changes in primal and dual variables x and y .
7. Determine the step length for the primal and dual variables and update them. Set $k = k + 1$ and go to Step 2.

IV. OTHER SOLVERS

The proposed method was compared to well-known solution methodologies for MINLP problems to test and validate it. Thus, a genetic algorithm [12, 13], and the GAMS [14] solvers BARON 7.2.5 and DICOPT++ were used for these purposes.

A. Genetic Algorithm (GA)

GAs are popular evolutionary programming techniques used for the solution of MINLP problems. These algorithms are based on simple genetic evolution, which takes place by means of three basic genetic operators: parent selection, crossover and mutation. The selection rule used here is a simple roulette-wheel selection; a single point crossover scheme is employed with high probabilities (0.7 to 0.95); and a mutation operator with a relatively small probability (0.0001 to 0.001) is applied to every bit of a chromosome. A fitness-based reinsertion is utilized to implement an elitist strategy, whereby the 10% most fit individuals are deterministically always propagated through successive generations.

If the slack bus voltage, capacitor outputs and transformer tap settings are defined as control variables U , and all the remaining variables are treated as state variables X , the original problem (1)-(5) can be rewritten as:

$$\min E(X, U) \quad (22)$$

$$\text{s.t. } G(X, U) = 0 \quad (23)$$

$$H(X, U) \leq 0 \quad (24)$$

$$U_{\min} \leq U \leq U_{\max} \quad (25)$$

The encoding and decoding schemes for control variables proposed in [12] are utilized here to solve (22)-(25) by means of a GA. Penalty terms are used to penalize for the violation of the constraints (24); this results in the following augmented objective function:

$$E_{\omega} = E(X, U) + \sum_j \omega_j Pen_j \quad (26)$$

$$Pen_j = |H_j(X, U)| \quad \text{if } H_j(X, U) > 0 \quad (27)$$

where Pen_j stands for a penalty function for an operating constraint H_j , and ω_j denotes the associated penalty factor.

Given an initial population for the problem represented by a chromosome, the computation of a fitness function may be carried out as follows [12]:

1. Decode the chromosome to determine the values of the control variables. The computed control vector should satisfy constraints (25) by design.
2. Solve the power-flow equations for each hour (23) to

calculate the state variables (the convergence tolerance was set to 10^{-6}).

3. Determine the violated operating constraints (24), and compute the augmented objective function (26).
4. Compute the fitness function using a linear ranking algorithm to transform the augmented objective function value into a measure of relative fitness [13].

A predefined number of generations is used as a termination criterion for the GA.

B. BARON

BARON is a popular GAMS solver for solving MINLP problems [14]. It is based on deterministic global optimization algorithms of the branch-and-bound type, which are guaranteed to provide global optima under fairly general assumptions. The nonlinear programming (NLP) and linear programming (LP) solvers required by BARON were chosen to be MINOS and CPLEX, respectively, given their robustness.

To be able to solve (1)-(5) using BARON, first, the power-flow equations had to be expressed in rectangular coordinate, since the program does not support trigonometric functions. Second, the discrete variables, i.e. transformer tap settings and capacitor outputs, had to be converted into integer variables. For transformer tap settings T_B , this can be readily accomplished as follows:

$$T_B = t_B \alpha_{step} + T_{B\min} \quad (28)$$

where $t_B = 1, 2, \dots, m$ is an integer that denotes the current tap position; α_{step} denotes the tap step size; and $T_{B\min}$ is the lower tap setting limit. A similar procedure can be used to represent capacitor outputs as integer variables.

C. DICOPT++

DICOPT is another ‘‘standard’’ MINLP solver in GAMS [14]. It is based on an extension of the equality relaxation outer-approximation algorithm, solving iteratively a series of NLP and mixed-integer programming (MIP) sub-problems. The NLP and MIP solvers used here, given their robustness, were MINOS and XA, respectively.

DICOPT++ can only handle binary and continuous variables. Therefore, to solve (1)-(5), the original discrete optimization variables, i.e. the transformer tap settings and capacitor outputs, should be converted to binary variables. This conversion can be readily realized by expressing the integer variables defined in (28) as a linear function of binary variables [17]; thus:

$$t_B = \sum_{l=0}^{s_b} \beta_l 2^l \quad (29)$$

where $s_b = \log_2(T_{B\max})$, $\beta_l = 0$ or 1 , and $T_{B\max}$ is the upper tap setting limit. A similar procedure can be used to represent capacitor outputs as binary variables. The power-flow equations can be expressed in its usual polar coordinate form in this case.

V. RESULTS

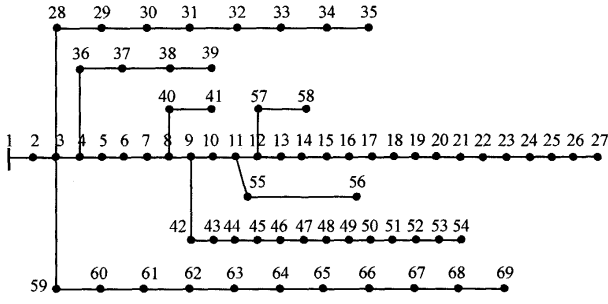


Fig.1. Schematic diagram of PG&E 69-bus system [18].

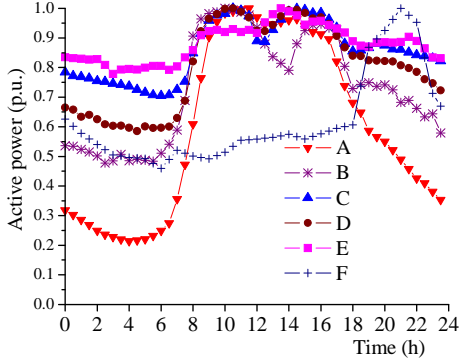


Fig.2. Typical daily load curves.

To demonstrate the effectiveness of the proposed method, the proposed algorithm and the GA, BARON and DICOPT solvers previously described were employed to obtain solutions for a reactive power dispatch and voltage control problem for the PG&E 69-bus distribution network [18], and for an actual 14-bus system in Luming, Guangzhou, China. The various solvers were implemented and tested in the following environments:

- The proposed algorithm was coded in Visual C++ and run on a Pentium IV, 2.8Gz computer (256 MB RAM).
- The GA was coded in MATLAB 7.0 and run on a Pentium IV, 3.0Gz computer (1 GB RAM).
- The BARON solver was run on an 8-virtual-processor MS-Windows IBM server.
- The DICOPT++ solver was run on a Pentium IV, 3.0Gz computer (1 GB RAM).

The use of different computational environments was due to the availability of the required software in the given piece of equipment.

A. PG&E 69-bus system

The PG&G 69-bus distribution test network is shown in Fig.1. The base power and base voltage are 10MVA and 12.66kV, respectively. The corresponding branch impedances and maximum daily active and reactive powers for all loads can be found in [18].

The system has 69 buses, 68 branches and 48 loads. Transformers at the 48 load buses are not represented, with the loads being modeled at the high-voltage side as constant power, neglecting the voltage dependence on the loads, which is a reasonable assumption given that the objective of the optimization process is hourly (steady-state) load voltage control. The capacitor banks are assumed to be installed in

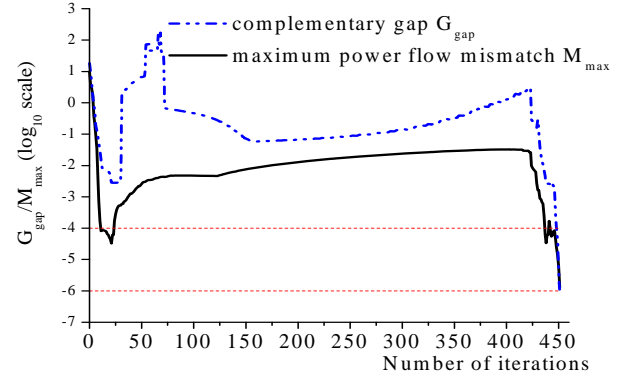


Fig.3. Maximum power-flow mismatch M_{\max} and complementary gap G_{gap} values for the proposed algorithm for the 69-bus system (MADSON = 7). The dashed lines depict the convergence tolerances ($M_{\max} < 10^{-6}$, $G_{\text{gap}} < 10^{-4}$).

TABLE I
PROPOSED ALGORITHM STATISTICS FOR THE 69-BUS SYSTEM

MADSON	Energy losses (MWh)	Number of iterations	CPU time (s)
7	2.60972	451	992.2
8	2.61058	89	195.8
9	2.61206	60	132.0
10	2.61059	35	77.0
11	2.61053	33	72.6
12	2.61030	31	68.2

TABLE II
NUMBER OF CAPACITOR SWITCHING OPERATIONS OBTAINED WITH THE PROPOSED ALGORITHM FOR THE 69-BUS SYSTEM

Bus	MADSON					
	7	8	9	10	11	12
9	4	4	8	8	8	8
19	4	2	2	2	2	2
31	2	2	2	4	2	2
37	5	6	7	6	7	7
40	6	4	8	8	8	8
47	4	4	4	4	4	4
52	6	6	6	6	6	6
55	5	7	7	7	7	7
57	2	2	2	2	2	2
65	4	4	4	4	4	4
TOTAL	42	41	50	51	50	50

Buses 9, 19, 31, 37, 40, 47, 52, 55, 57 and 65; Buses 37 and 52 have 3 and 4 sets of 0.3Mvar capacitors, respectively, while all other buses have only 2 sets of 0.3Mvar capacitors. The capacitor placement, which may be done using optimal placement methodologies (e.g. [19]), was simply determined here, without loss of generality as per the scope of the presented work, according to the load distribution on each feeder, since all loads are represented as constant power. The voltage at each bus is limited between 0.96 and 1.03. The daily load curves used for this system are shown in Fig. 2, and have been divided into 6 types, i.e. A to F, as illustrated in the figure; these load curves were obtained by normalizing real load power measurements in the city of Guangzhou, China, with respect to its maximum daily values. Buses 59, 60, 62-64, 66, 68 and 69 were represented as type A; Buses 42-44, 48, 50, 51, and 53-56 as type B; Buses 37-39 as type C; Buses 40, 41, 57 and 58 as type D; Buses 28, 29 and 33-35 as type E; and

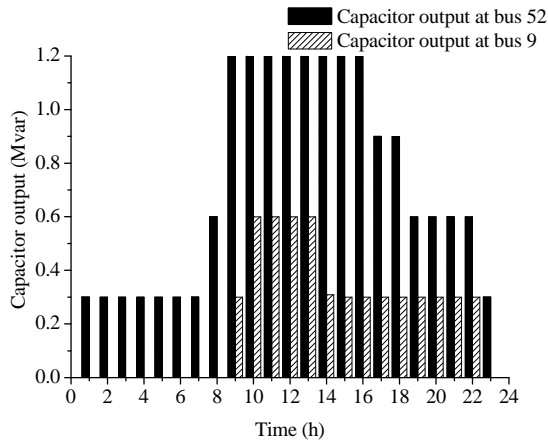


Fig.4. Optimal values obtained with the proposed algorithm for capacitor outputs for the 69-bus system (MADSON = 7).

TABLE III
GA STATISTICS FOR THE 69-BUS SYSTEM

MADSON	Energy losses (MWh)	CPU time (h)
7	2.71641	23.9
8	2.57422	23.2
9	2.60600	23.8
10	2.59125	24.2
11	2.60992	24.1
12	2.57392	23.6

Buses 6-18, 20-22, 24, 26 and 27 as type F. Constant power factors were assumed in all load buses.

1) *Proposed Algorithm Results:* Changing the MADSON from 1 to 15, it was observed that the proposed algorithm was not able to provide feasible solutions for $MADSON \leq 6$, due to the strict limits for switching operations of capacitors, whereas for $MADSON \geq 12$, both the solution and the iteration process remained unchanged. Thus, Table I illustrates the energy losses, number of iterations and execution time for MADSONs between 7 and 12, whereas Table II shows the capacitor switching operations in a day for the same MADSON values. The values of M_{max} and G_{gap} with respect to the number of iterations are illustrated in Fig. 3 for MADSON = 7.

From Fig.4, one can see that capacitor outputs at buses 9 and 52 are rounded off to their nearest discrete values for each hour with satisfactory accuracy. The larger the penalty factors, the better the discretization; for example, when penalty factors are set to 10,000, the error is less than 10^{-10} .

2) *GA:* For this test system, the control variables for each hour include one slack bus voltage and 10 capacitor outputs; thus, there are 11 control variables per hour, which yields 264 control variables per day. The chosen gene length for the slack bus voltage was 5 bits, and was treated as a continuous control, whereas the capacitor outputs are discrete values encoded using 2 or 3 bits. The GA population size was assumed to be

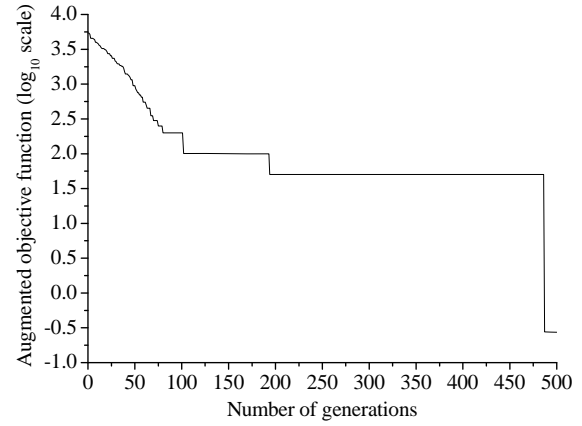


Fig.5. GA augmented objective function values for the 69-bus system.

TABLE IV
NUMBER OF CAPACITOR SWITCHING OPERATIONS OBTAINED
WITH A GA FOR THE 69-BUS SYSTEM

Bus	MADSON					
	7	8	9	10	11	12
9	0	8	4	10	10	10
19	4	4	4	4	2	4
31	6	6	8	8	8	12
37	6	6	8	10	10	8
40	6	4	6	6	10	12
47	6	6	6	8	8	6
52	6	8	6	10	8	8
55	2	2	0	4	2	4
57	6	8	8	8	8	8
65	4	4	2	2	2	2
TOTAL	46	56	52	70	68	74

300, and the maximum number of generations was set to 500; crossover and mutations were applied with probability values of 0.7 and 0.001, respectively. The penalty factors for the violation of bus voltage and switching operations were chosen to be 100 and 50, respectively. Only two runs were performed for each case examined, since it took more than 20 h to run one case using the developed GA in MATLAB; the results shown here correspond to the better of these two runs.

Tables III and IV show the energy loss, CPU times and capacitor switching operations for the same MADSONs used in the proposed algorithm. Figure 5 illustrates the evolution of augmented objective function value in (26) for a MADSON = 7. Table IV shows the capacitor switching operations in a day for different MADSON. Observe that the energy losses in this case are slightly less than those obtained with the proposed method in most of cases, as expected, since a GA will search for a global optimum; however, the proposed method is 86 to 1,246 times faster. Although the energy losses obtained from both algorithms are close, the switching sequences of capacitors in 24 hours are significantly different; in general, the total number of operations obtained with the proposed algorithm is smaller.

TABLE V
DICOPT AND PROPOSED METHOD ENERGY LOSS (MWh)
COMPARISON FOR THE 69-BUS SYSTEM

Hour	DICOPT Solver	Proposed Method	Hour	DICOPT Solver	Proposed method
0	0.05569	0.04012	12	0.19368	0.20490
1	0.04730	0.03420	13	0.19788	0.19110
2	0.03987	0.02930	14	0.20463	0.20240
3	0.03477	0.02540	15	0.19609	0.19070
4	0.03271	0.02400	16	0.18646	0.17930
5	0.03336	0.02440	17	0.15500	0.14770
6	0.03597	0.02620	18	0.11581	0.10760
7	0.05713	0.04240	19	0.09968	0.09940
8	0.13040	0.08886	20	0.09501	0.09490
9	0.17233	0.17080	21	0.08813	0.08480
10	0.21027	0.22260	22	0.07196	0.07150
11	0.26008	0.24680	23	0.07565	0.05480

3) *BARON*: In this case, with the power-flow equations expressed in rectangular coordinate, the discrete optimization problem is transformed into a standard MINLP problem with 240 discrete variables and 10 time-related inequality constraints; the number of continuous variables, equality constraints and functional inequality constraints are 3,312. No solution could be obtained using *BARON*, even when neglecting time-related inequality constraints and decomposing the problem into 24 smaller ones corresponding to each hour, i.e. solving single-hour optimization problems with no time-related inequality constraints. For the latter, for example, no solution could be obtained for the 12th-hour optimization sub-problem (after 217,300 iterations and 42 h of processing time).

4) *DICOPT++*: In this case, the discrete optimization problem is transformed into an MINLP problem with a standard polar-coordinate representation of the power-flow equations, yielding 504 binary variables, 3,312 continuous variables, 3,312 equality constraints, and 10 time-related inequality constraints. The maximum number of main iterations performed by *DICOPT* was set to 20.

No general solutions could be obtained with this solver, as the NLP sub-problems were always infeasible. However, when the time-related inequality constraints were ignored, solutions could be obtained for the resulting single-hour optimization problems. The energy losses at each hour obtained with this simplified model, and those obtained with the proposed method are presented in Table V. In this case, *DICOPT* yields a total energy loss for the day of 2.78986 MWh in 157.87 s of processing time, whereas the proposed method yields a total energy loss for the same day of 2.60493 MWh in 5.3 s of processing time. Even though *DICOPT* does yield an “exact” MINLP solution, whereas the proposed method yields an approximate one, the proposed method generates far better overall results than *DICOPT* in terms of both energy losses and execution time.

B. Luming System

The proposed voltage and reactive power control methodology has been in operation since 2003 in the Luming distribution system in the city of Guangzhou, China; thus, the

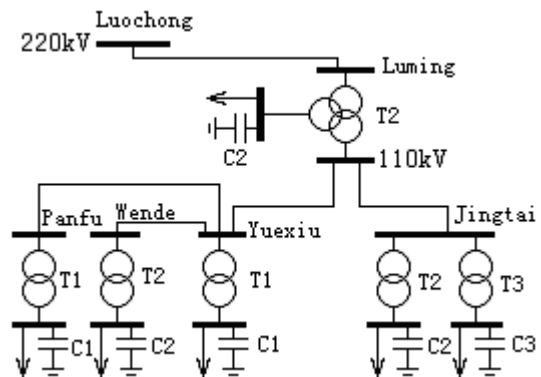


Fig. 6. Connection diagram of Luming 14-bus system.

TABLE VI
LUMING'S CONFIGURATION OF CAPACITORS

Capacitor	Number of capacitors	Capacity of each set (Mvar)
Luming C2	4	4.008
Jintai C2	2	3.0
Jintai C3	2	3.0
Panfu C1	1	3.3
Yuexiu C1	1	4.8
Wende C2	2	2.016

application of the proposed methodology to this system is explained here in some detail. The distribution system is located at the 220kV Luming substation, with five subsystems deriving from it as depicted in Fig. 6. Information can be exchanged by the SCADA systems between the main system and 5 subsystems. The proposed methodology was implemented at the main system level to carry out reactive power optimization calculations, so that an hourly optimal switching schedule of the LTC and capacitor banks is determined the day ahead. Based on this schedule, plus some additional calculations and a nine-zone diagram approach, the LTCs and capacitor banks are controlled in real-time.

As illustrated in Fig. 6, the Luming system is a 14-bus system consisting of a 220kV substation (Luming) and four 110kV substations (Jingtai, Panfu, Yuexiu and Wende). It includes 6 LTC transformers (Luming T2, Jingtai T2, Jingtai T3, Panfu T1, Yuexiu T1 and Wende T2) and 6 capacitor banks (Luming C2, Jingtai C2, Jingtai C3, Panfu C1, Yuexiu C1, and Wende C2), whose configuration are summarized in Table VI. The tap settings for Luming T2 are $1.03 \pm 8 \times 0.015$, and for the rest of the transformers these are $1 \pm 8 \times 0.015$. The lower and upper limits of voltages at each bus are set to 1.00 and 1.07, respectively. The real and reactive power losses of all transformers including active are represented in the model through proper resistance and reactance values of the transformers' equivalent circuits; transformer no-load losses are neglected. Given that the objective of the optimization process is basically hourly (steady-state) voltage control on the load side, all loads are represented using constant power load models, neglecting their voltage dependence. The active and reactive powers of the 6 depicted loads measured with a SCADA system on Sept. 10, 2001 are used here. The base power is 100MVA.

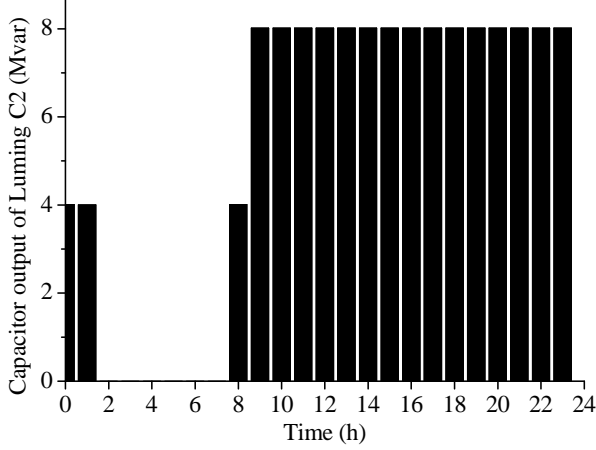


Fig.7. Optimal values of capacitor output obtained with the proposed algorithm for Luming C2 (MADSON = 8).

TABLE VII

PROPOSED ALGORITHM STATISTICS FOR LUMING SYSTEM

MADSON	Energy Losses (MWh)	Number of iteration	CPU time (s)
8	12.00970	402	44.22
9	12.01237	220	24.2
10	10.98918	60	6.6
11	10.99287	89	9.79
12	10.98930	67	7.37
13	10.99696	66	7.26
14	10.98901	46	5.06
15	10.98218	63	6.93
16	10.98219	51	5.61
17	10.99306	78	8.58
18	10.98708	52	5.72
19	10.98667	51	5.61
20	10.98670	52	5.72
21	10.97128	55	6.05
22	10.97975	75	8.25
23	10.99238	58	6.38
24	10.98433	56	6.16
25	10.98438	52	5.72
26	10.98434	51	5.61

1) *Proposed Algorithm*: Similarly to the previous sample system, reasonable solutions were obtained for a MADSON between 8 and 26, since no feasible solutions were obtained for a $MADSON \leq 7$ due to the strict limits for switching operations of capacitors and transformer LTCs, and the iteration process and results remained unchanged for a $MADSON \geq 26$. Table VII illustrates the energy losses, number of iterations and execution time obtained with the proposed method for different MADSON values. In Table VIII and Fig. 7, one can observe that the transformer tap settings and capacitor outputs are satisfactorily discretized, based on the previously defined discrete steps.

The numbers of transformer LTC switching operations for different MADSON values are presented in Table IX; as the MADSON increases, the number of operations tend to increase. Table X depicts the number of capacitor switchings; it remains unchanged for $MADSON \geq 10$. Finally, the values

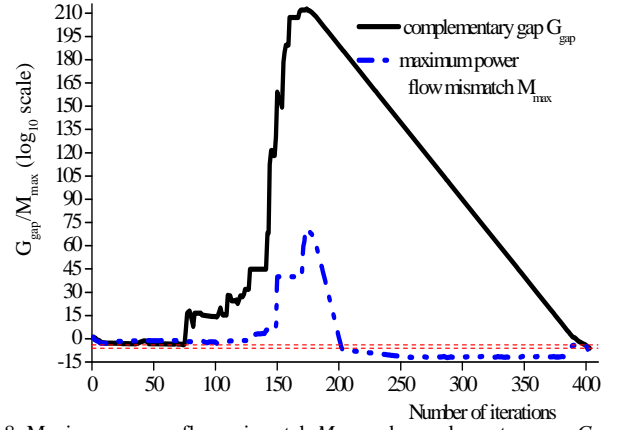


Fig.8. Maximum power-flow mismatch M_{max} and complementary gap G_{gap} for the proposed algorithm for the Luming system (MADSON = 8). The dashed lines depict the convergence tolerances ($M_{max} < 10^{-6}$, $G_{gap} < 10^{-4}$).

TABLE VIII

OPTIMAL TRANSFORMER TAP SETTINGS OF LUMING T2 OBTAINED WITH THE PROPOSED ALGORITHM (MADSON = 8)

Hour	Tap setting (p.u.)	Hour	Tap setting (p.u.)
00	1.00000	12	0.97001
01	1.00000	13	0.97001
02	1.00000	14	0.98497
03	1.00000	15	0.98497
04	1.00000	16	0.98497
05	0.98500	17	0.98497
06	0.98500	18	0.98498
07	1.00000	19	0.98500
08	1.00000	20	0.98500
09	0.98500	21	0.98500
10	0.98497	22	0.98500
11	0.97001	23	1.00000

TABLE IX

NUMBER OF TRANSFORMER LTC SWITCHING OPERATIONS OBTAINED WITH THE PROPOSED ALGORITHM

MADSON	Luming T2	Jintai T2	Jintai T3	Yuexiu T1	Panfu T1	Wende T2	TOTAL
8	6	0	0	2	2	2	12
9	8	0	0	2	2	2	14
10	2	2	2	4	6	6	22
11	4	2	4	4	6	10	30
12	6	2	4	4	6	10	32
13	8	2	4	4	6	8	32
14	12	2	4	4	6	12	40
15	10	2	4	6	6	6	34
16	10	2	4	4	6	10	36
17	14	2	4	4	6	10	40
18	16	2	4	4	6	8	40
19	10	2	4	4	6	10	36
20	10	2	4	4	6	10	36
21	20	2	4	4	6	6	42
22	14	2	4	4	6	6	36
23	14	2	4	8	6	10	44
24	18	2	4	8	6	10	48
25	18	2	4	8	6	10	48
26	18	2	4	8	6	10	48

of M_{max} and G_{gap} with respect to the number of iterations are illustrated in Fig. 3 for MADSON = 8.

2) *GA*: In this case, the control variables for each hour include a slack bus voltage, 6 capacitor outputs and 6 transformer tap settings; thus, there are 13 control variables

TABLE X
NUMBER OF CAPACITOR SWITCHING OPERATIONS OBTAINED
WITH THE PROPOSED ALGORITHM

MADSON	Luming C2	Jintai C2	Jintai C3	Yuexiu C1	Panfu C1	Wende C2	TOTAL
8	4	2	2	0	0	2	10
9	4	2	2	0	0	2	10
10	8	4	6	2	2	4	26

TABLE XI
GA STATISTICS FOR THE LUMING SYSTEM

MADSON	Energy losses (MWh)	CPU time (h)
24	13.51423	26.0
25	13.46813	26.8
26	10.82308	26.0

TABLE XII
NUMBER OF TRANSFORMER LTC SWITCHING OPERATIONS OBTAINED WITH GA

MADSON	Luming T2	Jintai T2	Jintai T3	Yuexiu T1	Panfu T1	Wende T2	TOTAL
24	20	24	22	22	14	24	126
25	24	24	22	22	14	24	130
26	10	24	16	26	24	26	126

TABLE XIII
NUMBER OF CAPACITOR SWITCHING OPERATIONS OBTAINED WITH GA

MADSON	Luming C2	Jintai C2	Jintai C3	Yuexiu C1	Panfu C1	Wende C2	TOTAL
24	10	4	4	6	6	2	32
25	8	6	4	8	10	8	44
26	16	4	4	2	0	2	28

per hour, yielding 312 control variables for the day. The gene length for the slack bus voltage was set to 8 bits and treated as a continuous control; the capacitor outputs take discrete values and were encoded using 1, 2 or 3 bits; finally, the transformer tap settings take 17 discrete values and were encoded using 5 bits. The GA population size was set to 4,500, the maximum number of generations to 500, and crossover and mutations were applied based on probability values of 0.95 and 0.0006, respectively. The penalty factors for the violation of bus voltage and switching operations were chosen to be 1000 and 50, respectively.

The GA did not yield feasible solutions for $MADSON \leq 23$. Table XI presents the energy losses and CPU times for different MADSON values; Fig. 9 illustrates the changes of the objective function value for a $MADSON = 24$; and Tables XII and XIII present the total number of daily switching operations of transformer LTCs and capacitors for the same MADSON values. Observe that the GA only yields solutions when the maximum limits on the number of switching operations are “relaxed”, i.e. for $MADSON \geq 24$, and in those cases, the energy losses and execution times are larger than those obtained with the proposed algorithm, especially CPU times; the same applies to the total number of switching operations, as in the previous example.

3) *BARON*: The discrete optimization problem was transformed into a standard MINLP problem with 288 discrete variables and 12 time-related inequality constraints; the numbers of continuous variables, equality constraints and functional inequality constraints are 672 in this case. As in the case of the 69-bus system, no solutions could be obtained.

4) *DICOPT++*: The discrete optimization problem was

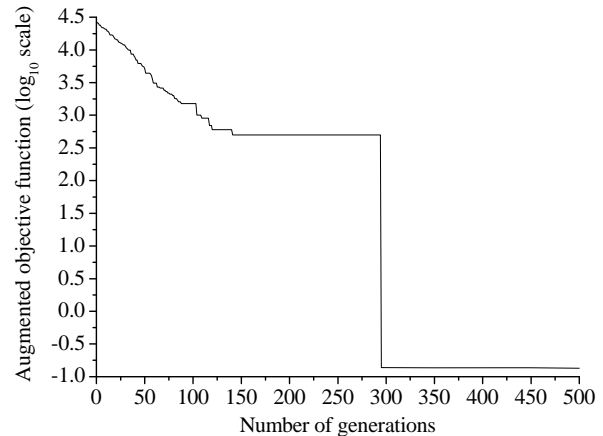


Fig.9. GA augmented objective function values for the Luming system.

TABLE XIV
DICOPT AND PROPOSED METHOD ENERGY LOSS (MWh) COMPARISON
FOR THE LUMING SYSTEM

Hour	DICOPT Solver	Proposed method	Hour	DICOPT Solver	Proposed method
0	0.2716	0.2631	12	0.7968	0.7991
1	0.2236	0.2107	13	0.7332	0.7347
2	0.1864	0.1821	14	0.6815	0.6860
3	0.1502	0.1469	15	0.6907	0.6933
4	0.1501	0.1499	16	0.6926	0.6968
5	0.1374	0.1354	17	0.6656	0.6706
6	0.1423	0.1412	18	0.5974	0.6039
7	0.1893	0.1810	19	0.5470	0.5515
8	0.3269	0.3229	20	0.5107	0.5042
9	0.5606	0.5637	21	0.5049	0.4889
10	0.6558	0.6599	22	0.4507	0.4431
11	0.7358	0.7365	23	0.4027	0.3885

transformed into another standard MINLP problem with 984 binary variables, 672 continuous variables, 672 equality constraints, and 12 time-related inequality constraints. The maximum number of main DICOPT iterations was set to 20, and various MINOS convergence parameters such as major/minor damping and penalties were chosen for the single-hour optimization sub-problems to obtain solutions.

Once more, a solution to the overall problem could not be found, due to the infeasibility of the NLP sub-problems; however, for single-hour optimizations, the results presented in Table XIV were obtained. Observe that DICOPT yields an “exact” discrete solution with a total daily energy loss of 11.0038 MWh in 24.3 s, while the proposed method provides an “approximate” discrete solution with a total energy loss of 10.95397 MWh in 1.6 s.

VI. CONCLUSIONS

A new and efficient method to solve the optimal daily reactive power dispatch and voltage control problem in distribution systems, considering limits on the number of daily switching operations for capacitors and transformer LTC, was proposed, discussed and tested here using realistic tests systems, highlighting and explaining in particular the practical application of the proposed technique in a real distribution system in China. The method is based on “rounding” all

discrete variables to their nearest discrete values with a desired accuracy, so that the inherent MINLP optimization problem can be transformed into a NLP problem that can be efficiently solved using an IPM.

The proposed technique was compared with “standard” MINLP solvers, namely, GA, BARON and DICOPT. The obtained results clearly show that the method yields accurate solutions in a fraction of the processing time needed by the other solvers, demonstrating the feasibility of implementing and applying this method in practice.

VII. APPENDIX

According to the Karush-Kuhn-Tucker conditions, the following follows from (14):

$$\begin{aligned} L_{x_{1(t)}} &= \nabla f_{x_{1(t)}} - \nabla g_{x_{1(t)}}^T y_{(t)} - y_{u1(t)} - y_{l1(t)} \\ &\quad - M_t y_n + \nu_{B(t)} (x_{1(t)} - x_{1(t)B}) = 0 \end{aligned} \quad (\text{A.1})$$

$$L_{x_{2(t)}} = \nabla f_{x_{2(t)}} - \nabla g_{x_{2(t)}}^T y_{(t)} - y_{u2(t)} - y_{l2(t)} = 0 \quad (\text{A.2})$$

$$L_{x_{3(t)}} = \nabla f_{x_{3(t)}} - \nabla g_{x_{3(t)}}^T y_{(t)} = 0 \quad (\text{A.3})$$

$$L_{y_{(t)}} = -g(x_{1(t)}, x_{2(t)}, x_{3(t)}) = 0 \quad (\text{A.4})$$

$$L_{y_{u1(t)}} = x_{1(t)} + s_{u1(t)} - x_{1(t)\max} = 0 \quad (\text{A.5})$$

$$L_{y_{l1(t)}} = x_{1(t)} - s_{l1(t)} - x_{1(t)\min} = 0 \quad (\text{A.6})$$

$$L_{y_{u2(t)}} = x_{2(t)} + s_{u2(t)} - x_{2(t)\max} = 0 \quad (\text{A.7})$$

$$L_{y_{l2(t)}} = x_{2(t)} - s_{l2(t)} - x_{2(t)\min} = 0 \quad (\text{A.8})$$

$$L_{s_{u1(t)}} = S_{u1(t)} Y_{u1(t)} e_1 + \mu e_1 = 0 \quad (\text{A.9})$$

$$L_{s_{l1(t)}} = S_{l1(t)} Y_{l1(t)} e_1 - \mu e_1 = 0 \quad (\text{A.10})$$

$$L_{s_{u2(t)}} = S_{u2(t)} Y_{u2(t)} e_2 + \mu e_2 = 0 \quad (\text{A.11})$$

$$L_{s_{l2(t)}} = S_{l2(t)} Y_{l2(t)} e_2 - \mu e_2 = 0 \quad (\text{A.12})$$

$$L_{y_n} = \sum_{t=0}^{N-1} |x_{1(t+1)} - x_{1(t)}| + s_n - S_{x_1} C_{x_1} = 0 \quad (\text{A.13})$$

$$L_{s_n} = S_n Y_n e_1 + \mu e_1 = 0 \quad (\text{A.14})$$

where $\nabla g_{x_{1(t)}}$, $\nabla g_{x_{2(t)}}$, and $\nabla g_{x_{3(t)}}$ are the gradients of $g(x_{1(t)}, x_{2(t)}, x_{3(t)})$; $\nu_{B(t)} \in \mathbb{R}^{p \times p}$ is a diagonal matrix with diagonal elements $\nu_{j(t)}$; $x_{1(t)B}$ is the vector that consists of the neighborhood centers of the discrete variables; $\nabla f_{x_{1(t)}}$, $\nabla f_{x_{2(t)}}$, and $\nabla f_{x_{3(t)}}$ are the gradients of $f(x_{1(t)}, x_{2(t)}, x_{3(t)})$; $e_1 = [1 \dots 1]^T \in \mathbb{R}^p$, and $e_2 = [1 \dots 1]^T \in \mathbb{R}^q$; and $Y_{u1(t)}$, $Y_{l1(t)}$, $Y_{u2(t)}$, $Y_{l2(t)}$, Y_n , $S_{u1(t)}$, $S_{l1(t)}$, $S_{u2(t)}$, $S_{l2(t)}$, and S_n are all diagonal matrices.

Using Newton’s method to solve (A.1)-(A.14), and after some rearrangements, one obtains the “reduced” correction equation (18) [20], in which all the slack variables and some Lagrangian multipliers have been eliminated, and where:

$$A_{(t,t)} = \begin{bmatrix} \bar{w}_{11(t)} & w_{12(t)} & w_{13(t)} & -\nabla g_{x_{1(t)}}^T \\ w_{21(t)} & \bar{w}_{22(t)} & w_{23(t)} & -\nabla g_{x_{2(t)}}^T \\ w_{31(t)} & w_{32(t)} & w_{33(t)} & -\nabla g_{x_{3(t)}}^T \\ -\nabla g_{x_{1(t)}} & -\nabla g_{x_{2(t)}} & -\nabla g_{x_{3(t)}} & 0 \end{bmatrix} \quad (\text{A.16})$$

$$\bar{w}_{11(t)} = w_{11(t)} + S_{l1(t)0}^{-1} Y_{l1(t)0} - S_{u1(t)0}^{-1} Y_{u1(t)0} + \nu_{B(t)} \quad (\text{A.17})$$

$$\bar{w}_{22(t)} = w_{22(t)} + S_{l2(t)0}^{-1} Y_{l2(t)0} - S_{u2(t)0}^{-1} Y_{u2(t)0} \quad (\text{A.18})$$

$$w_{kj(t)} = \nabla f_{x_{k(t)}, x_{j(t)}}^2 - \sum_{i=1}^{2n} y_{i(t)} \nabla g_{i x_{k(t)}, x_{j(t)}}^2 \quad (\text{A.19})$$

$$w_{jk(t)} = w_{kj(t)} \quad k, j = 1, 2, 3 \quad (\text{A.20})$$

$$\Delta z_{(t)} = \begin{bmatrix} \Delta x_{1(t)} & \Delta x_{2(t)} & \Delta x_{3(t)} & \Delta y_{(t)} \end{bmatrix}^T \quad (\text{A.21})$$

$$b_{(t)} = [B_{1(t)} \quad B_{2(t)} \quad -L_{x_{3(t)}0} \quad -L_{y_{(t)}0}]^T \quad (\text{A.22})$$

$$\begin{aligned} B_{1(t)} &= -L_{x_{1(t)}0} - S_{u1(t)0}^{-1} (L_{s_{u1(t)}0} - Y_{u1(t)0} L_{y_{u1(t)}0}) \\ &\quad - S_{l1(t)0}^{-1} (L_{s_{l1(t)}0} + Y_{l1(t)0} L_{y_{l1(t)}0}) \end{aligned} \quad (\text{A.23})$$

$$\begin{aligned} B_{2(t)} &= -L_{x_{2(t)}0} - S_{u2(t)0}^{-1} (L_{s_{u2(t)}0} - Y_{u2(t)0} L_{y_{u2(t)}0}) \\ &\quad - S_{l2(t)0}^{-1} (L_{s_{l2(t)}0} + Y_{l2(t)0} L_{y_{l2(t)}0}) \end{aligned} \quad (\text{A.24})$$

$$A_{(n,t)} = A_{(t,n)}^T = [-M_t \quad | \quad 0] \quad (\text{A.25})$$

$$A_{(n,n)} = Y_{n0}^{-1} S_{n0} I \quad (\text{A.26})$$

$$b_n = L_{y_n0} - Y_{n0}^{-1} L_{s_n0} \quad (\text{A.27})$$

and $\nabla^2 g_{x_{k(t)}, x_{j(t)}}$ and $\nabla^2 f_{x_{k(t)}, x_{j(t)}}$ are the corresponding Hessians of $g(x_{1(t)}, x_{2(t)}, x_{3(t)})$ and $f(x_{1(t)}, x_{2(t)}, x_{3(t)})$; $L_{x_{1(t)}0}$, $L_{x_{2(t)}0}$, $L_{x_{3(t)}0}$, $L_{y_{(t)}0}$, $L_{y_{u1(t)}0}$, $L_{y_{l1(t)}0}$, $L_{y_{u2(t)}0}$, $L_{y_{l2(t)}0}$, $L_{s_{u1(t)}0}$, $L_{s_{l1(t)}0}$, $L_{s_{u2(t)}0}$, $L_{s_{l2(t)}0}$, L_{y_n0} , and L_{s_n0} denote the residuals of (A.1)-(A.14); and $I \in \mathbb{R}^{p \times p}$ is an identity matrix.

VIII. ACKNOWLEDGEMENTS

The authors gratefully acknowledge the help of Mr. Kangling Qian and Ms. Fanghong Li from the Guangzhou Power Supply Bureau of Guangdong Power Grid Inc.

REFERENCES

- [1] Y. Y. Hsu and H. C. Kuo, “Dispatch of capacitors on distribution system using dynamic programming,” *IEEE Proceedings-Generation, Transmission and Distribution*, Vol. 140, pp. 433-438, June 1993.
- [2] F. C. Lu and Y. Y. Hsu, “Fuzzy dynamic programming approach to reactive power/voltage control in a distribution substation,” *IEEE Trans. Power Systems*, Vol. 12, pp. 681-688, May 1997.
- [3] Y. Y. Hsu and C. C. Yang, “A hybrid artificial neural network-dynamic programming approach for feeder capacitor scheduling,” *IEEE Trans. Power Systems*, Vol. 9, pp.1069-1075, May 1994.
- [4] Y. Y. Hsu and F. C. Lu, “A combined artificial neural network-fuzzy dynamic programming approach to reactive power/voltage control in a distribution substation,” *IEEE Trans. Power Systems*, Vol.13, pp.1265-1271, Nov. 1998.
- [5] R. H. Liang and C. K. Cheng, “Dispatch of main transformer ULTC and capacitors in a distribution system,” *IEEE Trans. Power Delivery*, Vol.16, pp. 625-630, Oct. 2001.
- [6] Y. Liu, P. Zhang, and X. Qiu, “Optimal volt/var control in distribution systems,” *Electrical Power & Energy Systems*, Vol. 24, pp. 271-276, May 2002.
- [7] Y. Deng, B. Zhang, and T. Tian, “A fictitious load algorithm and its applications to distribution network dynamic optimizations,” *Proceedings of Chinese Society of Electrical Engineering*, Vol. 16, pp. 241-244, July 1996.
- [8] Y. Deng, X. Ren, C. Zhao, and D. Zhao, “A heuristic and algorithmic combined approach for reactive power optimization with time-varying load demand in distribution systems,” *IEEE Trans. Power Systems*, Vol. 17, pp. 1068-1072, Nov. 2002.
- [9] Z. Hu, X. Wang, H. Chen, and G. A. Taylor, “Volt/Var Control in Distribution Systems Using a Time-Interval Based Approach,” *IEE Proceedings-Generation, Transmission and Distribution*, Vol. 150, pp. 548-554, Sept. 2003.
- [10] R. H. Liang and Y. S. Wang, “Fuzzy-based reactive power and voltage control in a distribution system,” *IEEE Trans. Power Delivery*, Vol. 18, pp. 610-618, April 2003.

- [11] M. B. Liu, S. K. Tso, and Y. Cheng, "An extended nonlinear primal-dual interior-point algorithm for reactive power optimization of large-scale power systems with discrete control variables," *IEEE Trans. Power Systems*, Vol. 17, pp. 982-991, Nov. 2002.
- [12] A. G. Bakirtzis, P. N. Biskas, C. E. Zoumas, and V. Petridis, "Optimal power-flow by enhanced genetic algorithm," *IEEE Trans. Power Systems*, Vol. 17, pp. 229-236, May 2002.
- [13] "Genetic algorithm toolbox for use with MATLAB," Department of Automatic Control and Systems Engineering, University of Sheffield, UK, 1994.
- [14] GAMS Development Corporation, "GAMS, the Solvers' Manual." Available online at <http://www.gams.com/solvers/allsolvers.pdf>.
- [15] V. H. Quintana and G. L. Torres, "Introduction to Interior-Point Methods," *IEEE PICA*, Tutorial, Santa Clara, CA, May 1999.
- [16] I. S. Duff, A. M. Erisman, and J. K. Reid, *Direct Methods for Sparse Matrices*, Oxford University Press, 1989.
- [17] J Riquelme-Santos, A. Troncoso-Lora, and A. Gomez-Exposito, "Finding improved local minima of power system optimization problems by interior-point methods," *IEEE Trans. Power Systems*, Vol. 18, pp. 238-244, Feb. 2003.
- [18] B. E. Baran and F. F. Wu, "Optimal capacitor placement on radial distribution systems," *IEEE Trans. Power Delivery*, Vol. 4, pp. 725-734, Jan. 1989.
- [19] H. N. Ng, M. M. A. Salama, and A. Y. Chikhani, "Capacitor allocation by approximate reasoning: fuzzy capacitor placement," *IEEE Trans. Power Delivery*, Vol. 15, pp. 393-398, Jan. 2000.
- [20] K. Xie and Y. H. Song, "Dynamic optimal power-flow by interior methods," *IEE Proceedings-Generation, Transmission and Distribution*, Vol. 148, pp. 76-84, Jan. 2001.

M. B. Liu received BS degree from Huazhong University of Science and Technology in 1985, MS degree from Harbin Institute of Technology in 1988, and PhD degree from Tsinghua University in 1992, all in Electrical Engineering. Currently, he is a Professor in the Electric Power College of South China University of Technology. From March 2006 to February 2007, he was a Visiting Professor at the Department of Electrical and Computer Engineering, University of Waterloo. His research interests are mainly in power system optimization, operation and control.

Claudio Cañizares (S'86, M'91, SM'00, F'07) received the Electrical Engineer degree from Escuela Politécnica Nacional (EPN), Quito-Ecuador, in 1984 where he held different teaching and administrative positions from 1983 to 1993. His MSc (1988) and PhD (1991) degrees in Electrical Engineering are from University of Wisconsin-Madison. He has been with the E&CE Department, University of Waterloo since 1993, where he has held various academic and administrative positions and is currently a Full Professor. His research activities concentrate in the study of stability, modeling, simulation, control, optimization and computational issues in power and energy systems within the context of competitive energy markets. Dr. Cañizares has been the recipient of various IEEE-PES Working Group awards, and has held and now holds several leadership positions in IEEE-PES technical subcommittees, as well as working groups and task forces.

W. Huang received BS degree in 2002 and MS degree in 2005 from South China University of Technology, all in Electrical Engineering. He is currently working at the Foshan Power Supply Bureau of Guangdong Power Grid Inc., Foshan, Guangdong, China.